


RESEARCH ARTICLE

Early movement restriction leads to enduring disorders in muscle and locomotion

Maxime Delcour¹; Vicky S. Massicotte²; Michaël Russier¹; H el ene Bras³; Julie Peyronnet³; Marie-H el ene Canu⁴; Florence Cayetanot³; Mary F. Barbe²; Jacques-Olivier Coq ^{1,3}

¹ Neurosciences Int egratives et Adaptatives, UMR 7260, CNRS, Aix-Marseille Universit e, Marseille, France.

² Department of Anatomy and Cell Biology, Lewis Katz School of Medicine, Temple University, Philadelphia, PA.

³ Institut de Neurosciences de la Timone, UMR 7289, CNRS, Aix-Marseille Universit e, Marseille, France.

⁴ Universit e de Lille, EA 7369 « Activit e Physique, Muscle et Sant e » - URePSSS - Unit e de Recherche Pluridisciplinaire Sport Sant e Soci et e, 59000 Lille, France

Keywords

cerebral palsy, DCD, disuse, musculoskeletal pathologies, post-activation depression, treadmill locomotion.

Corresponding author:

Dr J-O Coq, Institut de Neurosciences de la Timone (INT) UMR 7289, Team P3M, 27 Bd Jean Moulin, Campus Sant e Timone, 13385 Marseille Cedex 05, France
(E-mail: jacques-olivier.coq@univ-amu.fr)

Present address for M. Delcour: Equipe de Recherche en R eadaptation Sensorimotrice, Facult e de M edecine, D epartement de Physiologie, Universit e de Montr eal, C.P. 6128, Montr eal, Canada

Present address for M. Russier: Inserm UMR 1072, Unit e de Neurobiologie des Canaux Ioniques et de la Synapse, Facult e de M edecine Secteur Nord, Marseille Cedex, France

Received 26 September 2017

Accepted 9 February 2018

Published Online Article Accepted

13 February 2018

*Vicky Massicotte: Recently deceased (Feb 13, 2017). This author was a key contributor to the histological analyses and previously gave permission for co-authorship.

doi:10.1111/bpa.12594

Abstract

Motor control and body representation in the central nervous system (CNS) as well as musculoskeletal architecture and physiology are shaped during development by sensorimotor experience and feedback, but the emergence of locomotor disorders during maturation and their persistence over time remain a matter of debate in the absence of brain damage. By using transient immobilization of the hind limbs, we investigated the enduring impact of postnatal sensorimotor restriction (SMR) on gait and posture on treadmill, age-related changes in locomotion, musculoskeletal histopathology and Hoffmann reflex in adult rats without brain damage. SMR degrades most gait parameters and induces overextended knees and ankles, leading to digitigrade locomotion that resembles equinus. Based on variations in gait parameters, SMR appears to alter age-dependent plasticity of treadmill locomotion. SMR also leads to small but significantly decreased tibial bone length, chondromalacia, degenerative changes in the knee joint, gastrocnemius myofiber atrophy and muscle hyperreflexia, suggestive of spasticity. We showed that reduced and atypical patterns of motor outputs, and somatosensory inputs and feedback to the immature CNS, even in the absence of perinatal brain damage, play a pivotal role in the emergence of movement disorders and musculoskeletal pathologies, and in their persistence over time. Understanding how atypical sensorimotor development likely contributes to these degradations may guide effective rehabilitation treatments in children with either acquired (ie, with brain damage) or developmental (ie, without brain injury) motor disabilities.

INTRODUCTION

A common neurodevelopmental disorder and the main cause of physical disabilities in children is cerebral palsy (CP), a disorder thought to originate from perinatal brain damage. CP is a varied group of movement, posture and motor control disorders that are related to various muscle hypo- or overactivities, paresis, spasticity

and secondary musculoskeletal problems and associated to disturbances of somatosensation (25, 51). Without brain damage, difficulties or impairments in the planning, execution and control of body movements are considered developmental coordination disorders (DCD) and usually coexist with deficits in executive functions in 5%–6% of school-aged children (44). Children with autism spectrum disorder (ASD) also exhibit gross and fine motor

abnormalities, motor learning deficiencies and the persistence of primitive reflexes (11).

Most children developing these pathologies exhibit reduced physical activity and interactions with their environment (37, 57), as well as atypical motor development, detected as altered spontaneous or general movements (GMs) (20, 42). Briefly, during typical development, the repertoire of GMs in limbs increases in variation, fluency, amplitude and complexity into a continuous stream of small and elegant movements. In contrast, atypical GMs correspond to rigid and cramped-synchronized and stereotyped movements that exhibit limited fluency, complexity and variations with increasing age. Atypical motor development that leads in most cases to CP (with early brain damage) or DCD (without brain damage) is characterized by delays in the achievement of motor milestones, deviations in muscle tone and the persistence of infantile reactions and primitive reflexes (24, 33). Somatosensory feedback during movements is an integrated part of motor commands and contributes to drive muscle activation during gait; its participation in the emergence of gait disorders is questioned (18, 45, 46).

Even without brain damage, movement impairments, musculoskeletal pathologies, spasticity and related paresis can be induced in adults by either limb immobilization and disuse, or microgravity exposure (21, 39). For instance, a 2-week immobilization or a 4-week suspension of one leg in adults induces structural and functional muscle adaptations and increases the Hoffmann reflex (H-reflex), reflecting changes in spinal cord excitability in relation to decreased proprioceptive inputs to the sensorimotor circuitry (12, 13, 31). It is now understood that the development of movement repertoires, motor control and body representations in the sensorimotor circuitry are achieved through early spontaneous movements, sensorimotor experience and feedback in both humans (23, 24) and rodents (56). Although numerous studies examining the deleterious impact of transient immobilization or disuse have been conducted in adult animals (eg, Refs. 6, 7), very few have been performed during development. Hind limb unloading or restricted range of motion of young rodents induces slight yet transient gait changes (59, 61) and altered muscle physiology and phenotype (43, 52). In two prior studies, we used postnatal hind limb immobilization in neonates to achieve sensorimotor restriction (SMR) in combination with neonatal asphyxia to induce brain damage, in an attempt to explain the disabling movement disorders found in children with CP (15, 54). We extend those studies here to investigate the impact of postnatal SMR alone in rats on locomotion, musculoskeletal tissues and a possible relationship to spasticity. We postulate that limited amounts and abnormal patterns of somatosensory inputs during postnatal movement restriction may induce atypical development and refinement of the sensorimotor circuitry. Motor outputs and musculoskeletal structure and/or physiology may also be altered subsequently. We suppose that degraded musculoskeletal organization may also contribute to the persistence of impaired motor outputs and atypical somatosensory experiences in a self-perpetuating cycle.

METHODS

All experiments and animal use have been carried out in accordance with the guidelines laid down by NIH (NIH Publication #80-23) and EU Directive (2010/63/EU). The research involving

animals has been approved by the Direction Départementale des Services Vétérinaires—Préfecture des Bouches du Rhône, France (permit # C13-055-8JR).

Animals and hind limb immobilization

Sprague-Dawley rat pups of either sex from different litters were pseudo-randomly assigned to two groups: (i) a group subjected to transient hind limb immobilization from P1 to P28 for 16 h/day, thus producing SMR, and (ii) a control group (Cont). The feet of the SMR pups were first gently bound together with medical tape. Their hind limbs were then immobilized in extended position and taped to a cast, made of hand-moldable epoxy putty sticks (Figure 1). These casts were well tolerated by the pups and mothers, and allowed the pups to move at the hip, urinate, defecate and to receive maternal care. After casting, pups were returned to their mother and unrestrained littermates during the dark phase of day, corresponding to daily peaks of motor activity. During the day's light phase, the casts were removed so that pups could move freely for 8 h/day. After daily uncasting, the hind limb joints were passively moved through their full range of motion. The size of the casts was adapted to the growth of the rats from P1 to P28 (Figure 2). The casting was simulated in control rats without taping their hind limbs, so that all rats received comparable handling. The possible impact of stress induced by the casting and hind limb immobilization was minimized by similar handling of all rats (54). After weaning on P30, rats of the same sex were housed by 3 in standard plastic cages (26.5 × 42.5 × 18 cm) with sawdust on the floor and objects. The cages were kept in a room with controlled temperature and humidity, 12-h light-dark cycles (7:00 am to 7:00 pm) and food and water *ad libitum*.

We used 16 SMR (8 females and 8 males) and 19 control rats (10 females and 9 males). The rats that underwent gait assessment (SMR, $n = 10$; Cont, $n = 12$) at P30 and P65 were also used for analysis of hind limb musculoskeletal anatomy from P90 to P120. Another set of rats (SMR, $n = 6$; Cont, $n = 7$) was used for footprint measurements at P30 and *in vivo* electrophysiology at P60. Gait and footprint assessment was performed at the beginning of the light phase.



Figure 1. Young rat submitted to postnatal hind limb immobilization leading to SMR. To restrict movements, the feet of the pup were first tied together with medical tape and then attached to a cast made of epoxy stick. The proximal part of the hind limb was also taped to the cast, but the hip joint was free to move at the contrary to the knee, ankle and toe joints that were in an extended position during casting for 16 hours a day from P1 to P28.

3D kinematics during treadmill locomotion

Hind limb motion was acquired in 3D during automatic locomotion on a treadmill (Columbus Instruments, Simplex II, Columbus, OH) in the same animals at P30 and P65. Black permanent markers were used to place dots on the shaved skin of the back (iliac crest), hip (greater trochanter), knee, ankle (lateral malleolus) and 5th toe (metatarsophalangeal joint; Figure 3A,C) of rats. The 3D kinematics of the right hind limb dots were collected with two high-resolution CCD cameras (Basler A602fc, Ahrensburg, Germany) at a sampling rate of 250 Hz (Simi, Unterschleissheim, Germany). Briefly, offline video tracking (Simi) allowed us to reconstruct the 3D displacements of each joint of the leg (Figure 3A–D) to compute 24 parameters at each age (P30 vs. P65) and to reconstruct the movements in the form of bar diagrams (Figure 3B,D). The length and amplitude of the swing phase was normalized in each rat relative to the tibial bone length. Hind limb joint angles were measured on the flexor side of each joint and motion analyses were limited to the sagittal plane. We identified three main phases during the step cycle to calculate kinematic features: the beginning of the stance and swing, and the maximal height of the swing (MH swing; see 17 and Supporting Information Materials and Methods). Rats' locomotion abilities were assessed at two treadmill belt speeds (0.18 and 0.23 m/s). We present data from only one speed (0.23 m/s) since we found comparable changes with the two speeds.

To assess the impact of SMR on age-related plasticity of locomotion, we studied changes and variations in the kinematic parameters and joint angles, by using paired comparisons between ages P30 and P65 in controls vs. SMR rats. Kinematic variations in locomotion were determined using intra- and inter-group variations (averaged coefficient of variation or CV from each animal) for the

main kinematic parameters and joint angles through the different phases of the stride on treadmill. Given a sample of N observations for a gait parameter $X = \{x_1, \dots, x_N\}$, the CV was defined as,

$$CV(X) = \frac{\sqrt{1/N \sum_{i=1}^N (X_i - \bar{X})^2}}{\bar{X}}$$

Footprints

To assess the surface area of footprints and weight load during gait, rats at P30 were allowed to freely run across an illuminated glass walkway floor located in the corridor (width: 5 cm; length: 100 cm) of the Catwalk system (Noldus, Wageningen, The Netherlands). The footprints were digitized with a high-speed camera (10 frames/s). The maximal contact area (mm²) of the feet and weight load were automatically computed using the Catwalk system as rats crossed the walkway without any interruption or hitch during each of the three required runs (28). These two measures were normalized relative to each rat's weight.

In vivo electrophysiological recordings

The Hoffmann reflex is commonly used to assess primary (type Ia) afferents-mediated motor neuronal excitability (monosynaptic reflex loop) in individuals with spasticity (4, 5, 9). The H-reflex was measured in P60 rats from both groups under deep and constant anesthesia, induced first with isoflurane and then with ketamine (100 mg/kg i.p.) and maintained with supplementary doses of ketamine (20 mg/kg i.p.), as widely used (4, 5, 29). Rat temperature was maintained around 37°C with a thermal pad controlled by rectal temperature probe. A transcutaneous pair of stainless stimulating needle electrodes was inserted adjacent to the tibial nerve about 1 cm above the ankle. For EMG, a pair of stainless recording electrodes was inserted into the flexor digitorum brevis beneath the ankle and the reference electrode into the tail's skin (Supporting Information Figure S1). First, we stimulated the tibial nerve for 0.2 ms at 0.2 Hz with increasing current intensities until the M_{\max} stabilized, and determined the intensity required for a maximal H response. Tibial nerve was stimulated with trains of 20 stimulations at 0.2, 0.5, 1, 2 and 5 Hz with 2-minute intervals between each train to elicit post-activation depression (PAD). To determine the level of PAD at the different frequencies, we discarded responses to the first three stimulations required for the depression to occur. The M and H waves were rectified and the areas under the curves were measured. The H responses were expressed as percentages relative to the mean response at 0.2 Hz in the same series of measurements (4, 5).

Musculoskeletal histopathology analyses

After the electrophysiological cortical mapping, all rats from P90 to P120 received terminal anesthesia (thiopentobarbital, 150 mg/kg), before transcardial perfusion with fixative and collection of hind limbs, which were postfixed for 3 days. Hind limbs were X-rayed and the tibial bone assayed for length and then potential articular cartilage degenerative changes in knee joints after paraffin embedding, microtome sectioning and staining; gastrocnemius (GS) muscles were assayed for overall width, length and circumference

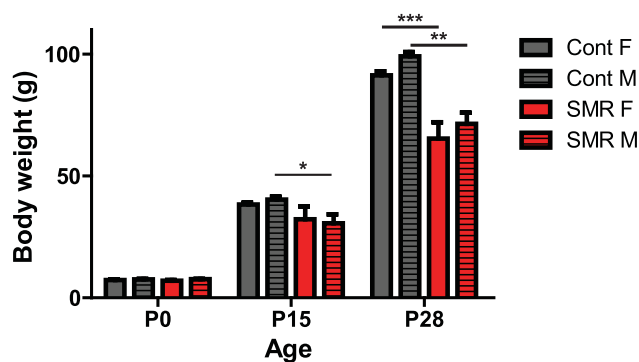


Figure 2. Influence of postnatal SMR and sex on body weight from birth to the end of SMR at P28. The body weight at birth (P0) did not differ between control and restrained rats ($F(1,30) = 0.16$; $P = 0.7$, ns) and both sexes ($F(1,30) = 2.61$; $P = 0.12$, ns). At P15, there was an effect of SMR on body weight ($F(1,30) = 7.78$; $P = 0.01$), but no effect of gender ($F(1,30) = 0.02$; $P = 0.89$, ns), nor interaction between group and gender. Tukey's *post hoc* comparisons showed that control males were bigger than SMR males (*, $P = 0.02$), but no differences between females. Similarly at P28, there was an effect of SMR on body weight ($F(1,30) = 53.53$; $P < 0.0001$), but no effect of gender ($F(1,30) = 3.74$; $P = 0.08$, ns), nor interaction between the two factors. Tukey's *post hoc* comparisons showed that both control females and males were bigger than SMR females (***, $P < 0.0001$) and males (**, $P = 0.007$), respectively. Mean \pm SEM. F, females; M, males.

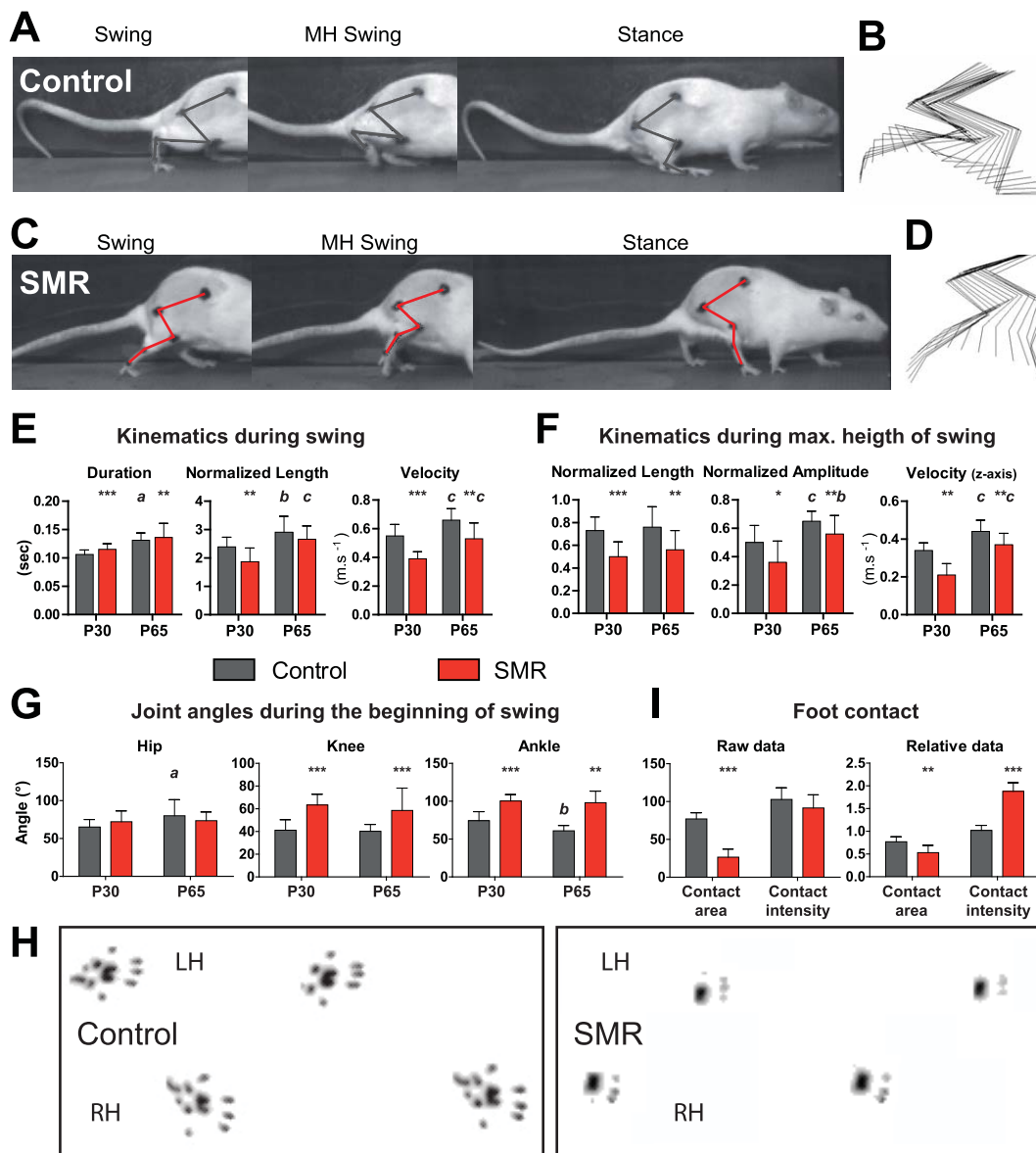


Figure 3. Illustration of 3D kinematics during treadmill locomotion at P65 and footprints in controls and rats that underwent sensorimotor restriction (SMR). **A,C.** Photographs of the three phases (beginning of the swing, maximal height of the swing—MH swing—and beginning of the stance) to show hind limb joint angles in representative control and SMR rats, respectively. **B,D.** Stick reconstruction of the right hind limb movements in the lateral plan during three representative swings in the same control and SMR rats as in A and C. **E–G.** Plots of the main changes in kinematic variables and joint angles induced by SMR during treadmill locomotion. The duration of the swing was longer in SMR rats than in control rats at P30 ($t = 5.54$; $d.f. = 20$; $P < 0.0001$) and P65 ($t = 2.69$; $d.f. = 21$; $P < 0.01$). At P30, the normalized lengths of the swing (E: $t = 2.99$; $d.f. = 20$; $P < 0.01$) and MH swing (F: $t = 4.26$; $d.f. = 20$; $P < 0.001$) phases were shorter in SMR rats compared with control rats while only that of the MH swing was still shorter after SMR at P65 (F: $t = 2.79$; $d.f. = 21$; $P < 0.01$). The normalized amplitude of the foot during the MH swing was lower in SMR than in control rats whether of the age (F: P30, $t = 2.42$; $d.f. = 20$; $P < 0.05$; P65, $t = 1.99$; $d.f. = 21$; $P < 0.05$). Velocities showed in E and F were reduced as well in SMR

rats compared with controls at both ages. The angle of the hip did not differ significantly between the two groups of rats whatever the phase and age, whereas the angles of the knee and ankle were larger in restrained rats than in controls for both ages at the beginning of the swing phase (G: knee at P30: $t = 6.14$; $d.f. = 20$; $P < 0.0001$; ankle at P30: $t = 3.04$; $d.f. = 20$; $P < 0.01$). **H.** Footprints of controls and SMR rats during gait in a walkway at P30. **I.** Plots of foot contact values in the walkway in control and SMR rats. The maximal foot contact area during weight bearing of SMR rats was much smaller than that of controls at P30 ($U = 0$; $P < 0.001$), even when the area was normalized relative to each rat's weight ($U = 6$; $P < 0.01$). The weight load of rats or foot contact intensity did not differ between both groups. After individual weight normalization, the relative mean intensity was greater in restrained rats compared with controls at P30 ($U = 0$; $P < 0.001$). Mean \pm SD. Note that all kinematic values as well as footprint data are indicated in Supporting Information Table S1. LH, left hind limb; RH, right hind limb. *P*-values: *, $P < 0.05$; **, $P < 0.01$; ***, $P < 0.0001$, SMR compared with control condition; a, $P < 0.05$; b, $P < 0.01$; c, $P < 0.0001$, P65 compared with P30.

and then cross sectional area of individual myofibers and numbers of Pax7-immunopositive cells after cryosectioning and staining; and the GS tendon was assayed for length using callipers; all as described briefly below and in detail in the Supporting Information Materials and Methods.

Tibial bone length (mm) was determined from X-rays of the hind limbs and used to normalize length and amplitude during locomotion in each corresponding rat. The GS muscle and tendon was separated from the bones. Callipers were used to measure the overall length and width of the GS muscle at its medial, lateral and intermediate portions and length of the GS tendon. The circumference of the GS muscle was also assayed. The GS muscles were cryosectioned at midbelly into 12 μm cross-sections, which were mounted onto charged slides (Fisher Plus) and dried overnight. Subsets of muscle sections were stained with hematoxylin and eosin (H&E). Cross-sectional areas of individual myofibers were measured (μm^2), in a blinded fashion, using a computerized bioquantification image analysis interfaced with a microscope and digital camera (see Supporting Information for more details). A mean of 146 myofibers were measured per muscle in three different non-adjacent sections (a mean of 48 myofibers per site) using 1000 \times magnification, bilaterally, by a blinded observer. Group means and standard errors (SEM) of the GS myofiber diameters were generated for both groups.

In order to examine for indices of muscle damage or regeneration, we immunostained GS muscle sections with anti-PAX7, a marker of satellite cells and proliferating myoblasts (3). For this, sections were blocked with 4% goat serum/PBS for 30 minutes at room temperature, before incubating overnight at 4°C with an anti-PAX7 antibody (anti-mouse PAX7; Developmental Studies Hybridoma Bank at the University of Iowa), diluted 1:10 in 2% bovine serum albumin/PBS. Slides were washed and then incubated with an appropriate Cy2-tagged (green label) secondary antibody (Jackson Immuno- Research Laboratories, PA) at a concentration of 1:200 in PBS for 2 h at room temperature. Images were captured using a digital camera mounted on an upright epifluorescent microscope interfaced with an image analysis software package (Bioquant, Nashville, TN). PAX7-positive cells were manually counted in a 0.003-mm² area at 1000 \times magnification.

Tibial bones were collected, decalcified and embedded in paraffin (See Supporting Information for more details). Mid-sagittal longitudinal sections (5 μm) were made of the tibia, femur and knee joint, using a microtome. Subsets of sections were stained with H&E, or with Safranin-O and fast green. The knee joint was assayed using a modified Mankin scoring system of structure, cellular abnormalities, matrix-safranin-O staining and tide-mark integrity. The methods used were as previously described (15) and as described in Supporting Information Materials and Methods.

Data analysis

Data normality and homogeneity of variances were determined with the Shapiro test, Bartlett test and var.test by using R (The R Foundation for Statistical Computing, Wien, Austria). We then applied either parametric (two-tailed and paired *t*-tests, and one-way ANOVAs with Tukey's *post hoc* comparisons and two-way ANOVAs) or nonparametric (Mann-Whitney, Wilcoxon and Chi square) tests using either R or Prism (GraphPad Software, CA). The investigators were blinded to rearing conditions throughout the different experimental sessions until statistical comparisons were performed.

RESULTS

Physical development

Body weight was measured at three time points: birth (P0), P15 and P28 at the end of hind limb immobilization (Figure 2). The weight at birth did not differ between both groups and sexes. By P15 and P28, the controls weighed more than the SMR rats ($P < 0.01$ and $P < 0.0001$, respectively), but did not differ by sex at either age (Figure 2). There was also no statistical interaction between group and sex at either age. In adult rats, the weight measures varied from 90 to 120 days of age, compromising reliable age-comparisons. However, the weight of P90–P120 females did differ between the two groups while the weight of control males was greater than that of SMR males ($P = 0.04$), suggestive of a differential weight gain more related to sex rather than SMR after its cessation.

SMR disturbs locomotor kinematics

At the end of hind limb immobilization (P28), qualitative observations revealed that SMR rats exhibited irregular step cycles, elevated hindquarters, gait disturbances related to their extended legs, compared with controls (Figure 3A–D; Supporting Information Videos S1 and S2). Some restrained rats dragged their feet and/or toes behind, so that their forelimbs propelled them. Despite slight improvements in gait and posture over time, these main deficits persisted into adulthood (from P30 to P65).

The cadence of locomotion on the treadmill did not differ between SMR and control rats at P30 and P65, nor did the cycle duration (Supporting Information Table S1). In contrast, the duration of the swing phase was longer in SMR rats than in controls at P30 ($P < 0.0001$) and P65 ($P < 0.01$; Figure 3E). The swing duration from the beginning to its maximal height (MH swing) was longer in SMR rats than in control rats at P30 ($P < 0.001$), but not at P65 ($P = 0.15$; ns). The duration of the stance phase (ie, weight bearing on treadmill) was reduced ($P < 0.05$), as was its length ($P < 0.05$) at P30 in SMR rats, compared with controls. Velocities were also reduced in SMR rats compared with controls at P30 and P65 (Figure 3E,F). At P30, the normalized lengths of the swing ($P < 0.01$) and MH swing ($P < 0.001$) phases were shorter in SMR, compared with controls, while only the MH swing remained shorter in SMR by P65 ($P < 0.01$; Figure 3E,F). The normalized amplitude (ie, height) of the foot during the MH swing phase was lower in SMR than in control rats, regardless of age (P30/P65: $P < 0.05$; Figure 2F). Comparable results for raw data on lengths and amplitude were found (Supporting Information Table S1).

The hip angle did not differ between groups regardless of the phase or age. In contrast, the knee and ankle angles were much larger (ie, overextension) in SMR rats than in controls for both ages at the beginning of the swing phase (eg, knee at P30: $P < 0.0001$; ankle at P30: $P < 0.01$; Figure 3G) and MH swing (knee at P30: $P < 0.0001$; ankle at P30: $P < 0.0001$). At the beginning of the stance phase, only the angle of the ankle was larger in SMR rats at both ages (eg, P30: $P < 0.001$; Supporting Information Table S1). Two-way ANOVA showed no effect of sex on 45 gait parameters out of 48, only swing duration (P30: $P = 0.04$), z-axis velocity of the foot (P30: $P < 0.05$) and cycle duration (P65: $P = 0.03$) showed sex-related differences.

Table 1. Averaged CV for kinematic parameters in controls and rats that underwent postnatal SMR at different ages (P30 and P65) for a treadmill speed of 0.23 m/s. To ease clarity, bold numbers point out differences between SMR and control rats at the same age. Mean \pm SD. AC, Age-related changes in variation; \uparrow or \downarrow or =, increase or decrease or unchanged between P30 and P65 in each group of rats.

		P30		AC	P65		AC
		Controls	SMR		Controls	SMR	
Swing	Duration (s)	0.193 \pm 0.018	0.128 \pm 0.084	\downarrow^e	0.146 \pm 0.039	0.229 \pm 0.060 ^c	=
	Length (m)	0.272 \pm 0.040	0.281 \pm 0.087	\downarrow^e	0.166 \pm 0.052	0.229 \pm 0.077 ^a	\downarrow^d
	Velocity (x-axis, m/s)	0.209 \pm 0.071	0.320 \pm 0.087 ^c	\downarrow^d	0.161 \pm 0.039	0.224 \pm 0.080 ^a	\downarrow^d
	Hip angle (°)	0.121 \pm 0.044	0.082 \pm 0.032 ^a	\downarrow^f	0.058 \pm 0.015	0.049 \pm 0.013	\downarrow^d
	Knee angle (°)	0.215 \pm 0.053	0.110 \pm 0.029 ^c	\downarrow^f	0.133 \pm 0.030	0.101 \pm 0.042 ^a	=
Maximal height of the swing	Ankle angle (°)	0.165 \pm 0.039	0.112 \pm 0.021 ^c	\downarrow^e	0.126 \pm 0.022	0.108 \pm 0.025 ^a	=
	Duration (s)	0.171 \pm 0.077	0.453 \pm 0.185 ^c	=	0.158 \pm 0.046	0.375 \pm 0.160 ^c	=
	Length (m)	0.307 \pm 0.125	0.562 \pm 0.162 ^c	=	0.317 \pm 0.091	0.492 \pm 0.172 ^b	=
	Velocity (x-axis, m/s)	0.217 \pm 0.075	0.390 \pm 0.128 ^c	=	0.234 \pm 0.070	0.292 \pm 0.085 ^a	\downarrow^d
	Amplitude (z-axis, m)	0.200 \pm 0.045	0.331 \pm 0.137 ^b	\downarrow^d	0.162 \pm 0.029	0.200 \pm 0.067 ^a	\downarrow^e
	Velocity (z-axis, m/s)	0.222 \pm 0.065	0.694 \pm 0.503 ^b	\downarrow^t	0.186 \pm 0.032	0.345 \pm 0.0142 ^c	\downarrow^d
	Hip angle (°)	0.126 \pm 0.044	0.078 \pm 0.032 ^b	\downarrow^f	0.052 \pm 0.016	0.049 \pm 0.010	\downarrow^e
	Knee angle (°)	0.201 \pm 0.042	0.108 \pm 0.036 ^c	\downarrow^f	0.120 \pm 0.034	0.105 \pm 0.046	=
	Ankle angle (°)	0.225 \pm 0.060	0.092 \pm 0.018 ^c	=	0.197 \pm 0.085	0.085 \pm 0.026 ^c	=
	Stance	Duration (s)	0.271 \pm 0.103	0.353 \pm 0.155^t	=	0.256 \pm 0.103	0.285 \pm 0.090
Length (m)		0.307 \pm 0.115	0.407 \pm 0.187	=	0.288 \pm 0.121	0.314 \pm 0.119	=
Hip angle (°)		0.114 \pm 0.035	0.080 \pm 0.028 ^b	\downarrow^f	0.051 \pm 0.017	0.059 \pm 0.016	\downarrow^t
Knee angle (°)		0.138 \pm 0.035	0.117 \pm 0.023^t	\downarrow^e	0.100 \pm 0.021	0.090 \pm 0.032	\downarrow^d
Ankle angle (°)		0.170 \pm 0.043	0.100 \pm 0.025 ^c	=	0.153 \pm 0.040	0.092 \pm 0.028 ^c	=

^aDifferent from controls, $P < 0.05$.

^bDifferent from controls, $P < 0.01$.

^cDifferent from controls, $P < 0.001$.

^dDifferent from P30, $P < 0.05$.

^eDifferent from P30, $P < 0.01$.

^fDifferent from P30, $P < 0.001$.

^tTendency, $0.05 < P < 0.10$.

In addition, the maximal foot contact area during weight bearing (ie, footprint surface) in SMR rats was much smaller than that of controls at P30 ($P < 0.001$), even when the area was normalized relative to each rat's weight ($P < 0.01$; Figure 3I,H; Supporting Information Table S1). Control rats displayed a plantigrade locomotion (48), characterized by footprints that encompassed the medial and/or distal phalanges of all toes and all plantar pads. In contrast, the footprints of SMR rats were limited to the distal phalanges toes 2–4 and contiguous distal plantar pads, each hallmarks of a digitigrade locomotion (Figure 3H). The weight load or foot contact intensity did not differ between the groups. However, when the values were normalized relative to the corresponding rat's weight, the relative mean intensity was much larger in SMR rats at P30, compared with controls ($P < 0.001$; Figure 3I).

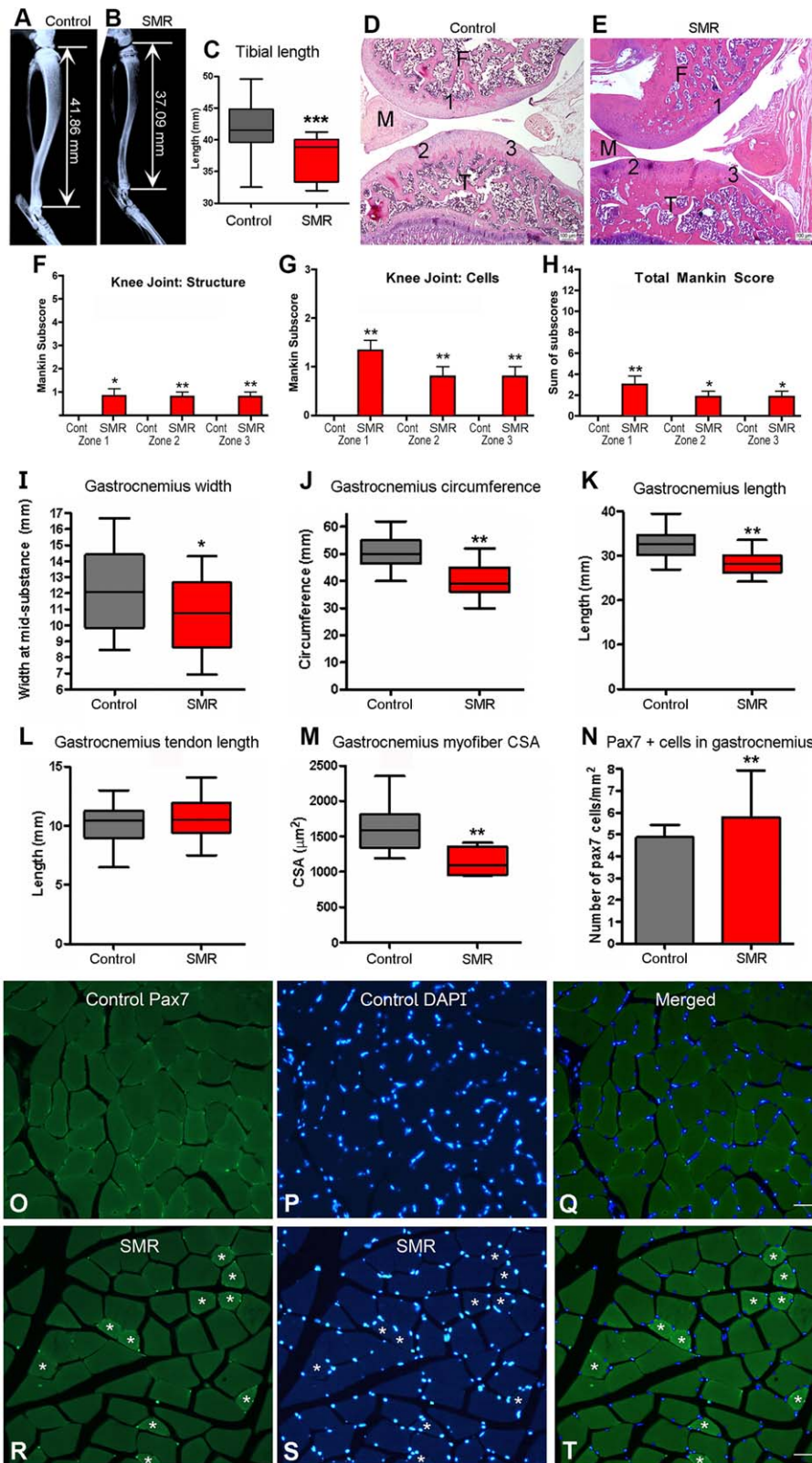
Age-related changes and variations in locomotion parameters after SMR

The majority of the kinematic and angle parameters (54%, 13/24) were persistently modified in SMR rats (at both P30 and P65), compared with controls, while 25% (6/24) of the parameters were unchanged after SMR regardless of age, and 21% (5/24) of the parameters were only altered at P30, suggesting enduring impact of SMR on half of the locomotion parameters beyond the cessation of SMR on half of the locomotion parameters beyond the cessation of the hind limb immobilization.

Intra- and inter-group variations (averaged CV) were assessed for the kinematic parameters and joint angles and were compared between P30 and P65 to evaluate age-related plasticity of gait (17, 23, 26). In controls, most (12/19) of the CVs of the kinematic parameters and joint angles decreased from P30 to P65, although a few remained constant (7/19). In contrast, in SMR rats, as many CVs decreased (9/19) as remained unchanged (10/19) over time (see AC in Table 1), suggestive of subtle differences in the gait maturation angles between the two groups of rats. However, the mean CVs and corresponding SDs of the kinematic parameters evolved differently over time than those for joint angles in both groups of rats. For the kinematic parameters, most of the CVs and SDs were greater in SMR rats than in controls at both P30 and P65. In contrast, most of the CVs and SDs of joint angles were reduced or comparable in SMR rats, regardless of age (Table 1). For example, the CVs of the ankle joint were reduced in SMR rats relative to controls, at both ages and all gait phases examined (Table 1). We found no specific impact of sex on the CVs of all gait parameters.

Musculoskeletal histopathology related to SMR

The experimenters were able to passively move the hind limb joints through their full range of motion, despite some resistance, during the daily uncasting period from P1 to P28 and after casting cessation during treadmill testing.



Tissues were collected post-euthanasia and examined for any evidence of histopathology. We first examined the tibia radiologically and observed reductions in its length after SMR ($P < 0.0001$;

Figure 4A–C). There was also a qualitative reduction in tibial bone radiopacity in SMR rats compared with control rats (Figure 4A,B), suggestive of reduced bone density in SMR rats. We next examined

Figure 4. Morphological assessment of the tibial bone, femoral and knee joints, and GS muscle in control rats and rats submitted to postnatal sensorimotor restriction (SMR). **A,B.** X-ray images of tibial bones and corresponding tibia length in representative control and SMR rats. **C.** The length of the tibial bone was reduced in SMR rats compared with controls ($t = 5.52$; d.f. = 63; $P < 0.0001$). **D.** Control knee at low power showing normal staining of articular cartilages and well defined basophilic tidemarks. **E.** A SMR knee, which even at low power, displays a general loss of the cartilage tidemark, a basophilic line marking the boundary between calcified matrix and uncalcified cartilage. Scale bars = 100 μm . **F,G.** Mankin scores of both structural and cellular changes are shown for zones 1–3, showed in D and E. **I–N.** Plots of various measures of the GS in the two groups of rats. **I.** The width of the GS was reduced in SMR rats ($t = 2.52$; d.f. = 63; $P = 0.01$). **J.** The circumference of the GS was reduced after SMR

($t = 7.05$; d.f. = 59; $P < 0.001$). **K.** The length of the GS was also reduced after SMR ($t = 6.25$; d.f. = 63; $P < 0.001$). **L.** The length of the GS tendon was comparable between restrained and control rats ($t = 0.86$; d.f. = 63; $p = 0.39$, ns). **M.** The cross-sectional areas (CSA) of GS myofibers were reduced after SMR ($t = 2.91$; d.f. = 18; $P = 0.005$). **N.** SMR increased the numbers of PAX7-positive cells in the GS myofibers ($t = 5.45$; d.f. = 9; $P = 0.0004$). **O,R.** Images of PAX7-positive cells in the GS of both groups. Note the presence of smaller myofibers in SMR rats depicted by white asterisks. **P,S.** Images of DAPI-positive cells in the GS of both groups of rats. **Q,T.** Merged pictures of PAX7 and DAPI stainings in control and SMR rats, respectively. Scale bars = 50 μm . (C,I–N) Mean \pm SD. (F–H) Mean \pm SEM. *, $P < 0.05$; **, $P < 0.01$; ***, $P < 0.0001$, compared with controls.

the knee joints and observed in SMR rats, but not in controls, mild to moderate degenerative changes in the femoral and tibial knee articular cartilages, subchondral bone and growth plates, indicative of mild to moderate chondromalacia in the knee joint (Figure 4D–H, Supporting Information Figure S2).

Several focal sites of cartilage structural damage were observed in all SMR rats examined. Histologically, there was a general loss of the cartilage tidemark, a basophilic line marking the boundary between calcified matrix and uncalcified cartilage in all SMR rats compared with controls (Figure 4D,E) and a significant loss of articular cartilage on the femoral side of SMR rats, compared with controls (Figure 4D,E; Supporting Information Figure S2A,B,E). Each of these changes contributed to an increased structure change in SMR rats, compared with controls, using the Mankin scoring system of articular cartilage degeneration (Figure 4F). Also in SMR rats, chondrocytes of the articular cartilage displayed hypercellularity and clustering in the tibial cartilage (Figure 4G; Supporting Information Figure S2C,D). Specifically, with regards to articular cartilage region, there were small but significant structural and cellular changes in SMR rats, compared with control rats, in zone 1 (mid-femoral articular cartilage; zones are indicated in Figure 3D,E), zone 2 (medial-tibial plateau articular cartilage) and zone 3 (lateral tibial plateau articular cartilage), but not in zone 4 (medial meniscus; data not shown). When subscores of knee joint degeneration were summed into a total Mankin score, mild but significant changes were present in zones 1–3 of SMR rats, compared with controls (Figure 4H). Additionally, the tibial epiphyseal plate in several SMR rats showed moderate abnormalities (Supporting Information Figure S2F).

GS muscles were assessed for morphological changes and showed reductions in width ($P = 0.01$), circumference ($P < 0.001$) and length ($P < 0.001$) in SMR rats compared with control rats (Figure 4I–K). In contrast, the length of the GS tendon did not differ between the two groups (Figure 4L). Although the number of myofibers in the GS did not differ (data not shown; $P = 0.16$, ns), the cross-sectional areas (CSA) of GS myofibers were reduced in SMR rats, compared with controls ($P = 0.005$; Figure 4M). Representative images of cross-sectional myofibers are shown in Figure 4O–T (note smaller myofibers in SMR rats indicated by white asterisks; Figure 4R–T). Comparable reductions in myofiber size were also observed in rectus femoris and tibialis anterior muscles in SMR rats (data not shown). Sectioned GS muscles also showed

increased numbers of PAX7-positive cells, a marker of satellite cells and proliferating myoblasts, in SMR rats, compared with control rats ($P = 0.0004$; Figure 4N,O–T), suggestive of ongoing regeneration processes. In addition, we found no effect of sex on the different musculoskeletal measures, except for GS width ($P = 0.002$).

Post-activation depression of reflex loops

To evaluate the presence of spasticity after SMR, corresponding to hyperexcitability in the spinal circuitry, we assessed the changes in the Hoffmann reflex (H-reflex; Figure 5A; Supporting Information Figure S1) (4, 5, 27). In adult control rats, the H-reflex was depressed by repeated nerve stimulation at frequencies increasing from 0.2 Hz to 5 Hz ($P < 0.0001$; Figure 5B), corresponding to PAD (4, 5). In contrast, the PAD was reduced in adult SMR rats ($P < 0.0001$), as illustrated by the lack of significant differences of the monosynaptic H-reflex with increasing frequencies (Figure 5B). When we compared the H-reflex PAD between controls and SMR rats, we found significant effects of both increasing frequencies ($P < 0.0001$) and between-groups comparison ($P < 0.0001$). In addition, for each stimulation frequency from 0.2 Hz to 5 Hz, the H-reflex PAD was decreased in SMR vs. control rats (see Tukey's *post hoc* comparisons *a* to *c* in Figure 5B), suggesting the presence of spasticity at one month after cessation of SMR, as previously demonstrated (4, 5). There was no effect of sex on PAD.

DISCUSSION

This is the first investigation of the enduring impact of early atypical sensorimotor experience (SMR) by using postnatal movement restriction on gait and posture, variations of locomotion parameters to assess age-dependent process, musculoskeletal histopathology and muscle hyperreflexia. Compared with controls, SMR induced: (i) severely degraded gait and posture on a treadmill likely because of knee-ankle overextension that persisted over time as well as smaller footprints; (ii) increased variations of kinematics yet reduced joint angle variations that persisted over time; (iii) reduced tibial bone length and density, increased knee joint degenerative changes and GS myofiber atrophy, yet also evidence of muscle regeneration and (iv) muscle hyperreflexia assessed by using PAD, suggestive of spasticity.

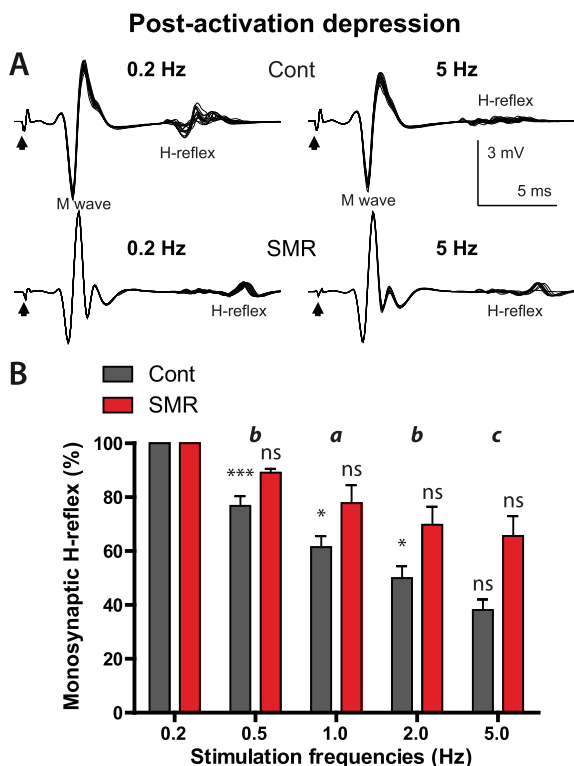


Figure 5. Decreased PAD of the Hoffmann reflex measured *in vivo* in adult control and SMR rats. **A.** Representative traces of M and H waves elicited at 0.2 Hz (used as reference) and 5 Hz in both groups of rats. Typical EMGs exhibit two responses: an initial M wave resulting from the direct activation of motoneuron axons by the tibial nerve stimulation leading to a muscle contraction and a delayed H wave resulting from the monosynaptic activation of motoneurons by Ia afferents activity driven by the electrical stimulation, corresponding to the Hoffmann reflex (H-reflex). Note the constant level of the M wave whether of the frequency of stimulation in both groups of rats, while the H-reflex magnitude decreased with increasing frequency in the control rat, but not in the SMR rat. **B.** Depression of the H-reflex (PAD), expressed as percentages, over consecutive stimulations from 0.2 Hz (set as reference = 100%) to 5 Hz in controls ($F(1,4) = 47.9$; $P < 0.0001$) and Tukey's *post hoc* comparisons: * $P < 0.05$; *** $P < 0.0001$; ns, non-significant differences) while the H-reflex did not reduce significantly between consecutive frequencies of stimulation in SMR rats ($F(1,4) = 6.9$; $P < 0.0001$) and Tukey's *post hoc* comparisons: ns, non-significant). When we compared the H-reflex PAD between controls and SMR rats, we found significant effects of both stimulation frequencies ($F(1,4) = 40.2$; $P < 0.0001$) and between-groups comparison ($F(1,4) = 32.4$; $P < 0.0001$), as well as a significant interaction between groups and stimulation frequencies ($F(2,4) = 32.4$; $P = 0.02$). In addition, Tukey's *post hoc* comparisons (a, $P < 0.05$; b, $P < 0.01$; c, $P < 0.0001$) show decreased PAD for each stimulation frequency from 0.5 to 5 Hz between adult SMR and control rats. The arrows depict the stimulation artefacts.

SMR degrades gait and posture on treadmill

Although cadence and stride duration did not differ, the length, amplitude, corresponding normalized values and velocities of the foot were lower overall in SMR rats than in controls, reductions that persisted over time. SMR induced significant knee and ankle

overextension during automatic locomotion, especially in the ankle in all gait phases examined, whereas the hip angle was unchanged. An absence of changes in the hip angles after SMR was likely because of the preservation of hip movements during the developmental hind limb immobilization. In contrast, during weight bearing on the treadmill (ie, stance phase), only the ankle was overextended at all age points, showing persistent over-plantarflexion. Using the same procedures and duration of early hind limb immobilization, previous studies also reported gait and posture deficits that persisted even after cessation of immobilization (34, 35, 54). Such deficits appeared to contribute to impairments observed during acrobatic walking on a narrow beam, horizontal ladder and rotarod testing (35, 54). The absence of proprioceptive feedback from muscle spindles in transgenic mice also degrades the temporal patterns of gait (1). In our study, footprint analysis showed a switch from plantigrade locomotion in controls to digitigrade locomotion and increased intensities of foot contact after SMR. The latter suggests differences in tactile and proprioceptive inputs to the central nervous system (CNS) during and beyond movement restriction. Taken together, these results emphasize the deleterious impact of disturbed proprioceptive feedback on the development and control of gait and posture.

In addition, SMR rats appeared to develop locomotor and postural features that recapitulate “toe walking” or true equinus, characterized by ankle overextension and full knee extension (49). True pes equinus is the most common symptom seen in spastic diplegic children and adults with CP (49). SMR rats exhibited reduced gait velocity and shorter stride lengths, also observed in subjects with spastic CP (8, 16, 47). The interplay between gait disorders and the presence of spasticity and muscle overactivities related to neural plasticity has been attested in several studies, although the degree and direction of causality is still under debate (8, 16, 18, 21, 22, 49).

Age-related plasticity of gait kinematics and their variations after SMR

Concerning the enduring effects of SMR, hind limb unloading in adult rats induces transient locomotor and muscular changes (6, 7). Postnatal immobilization of one leg induces only a “slight extension bias” of the immobilized leg and an increase in the swing duration that did not persist beyond one or two weeks after immobilization termination (61). In contrast, bilateral SMR from P1 through P28 for 16 h/day led to locomotor disorders that persisted one month after cessation of movement restriction.

We use the term “variation” (ie, coefficient of variation) for the evaluation of the range of motor repertoires available in rats during maturation and age-dependent plasticity of gait, different from “variability” that corresponds to the ability for the sensorimotor circuitry to select the most appropriate motor solution within the available motor repertoire (24). Infants with typical development produce a large and rich repertoire of spontaneous movements (ie, GM) with abundant variation and increasing complexity with time, representative of various motor possibilities. In a later phase of adaptive variability, sensorimotor experience and somatosensory feedback guide the sensorimotor circuitry to select the most adapted motor behaviors (24). Then, typical mature gait becomes characterized by low variation and a high degree of symmetry from stride-to-stride. In contrast, children with CP, DCD or ASD exhibiting atypical motor development display scarce, monotonous and

stereotypical patterns of GMs that show a lack of variation, complexity and fluency over time (8, 23, 24, 26, 42, 47).

In the present study, the variations for most of the kinematics and joint angles decreased in control rats from P30 to P65, corresponding to typical gait plasticity in rats (20) or in humans (24, 26). In contrast, SMR led to increased variations in gait kinematic parameters but reduced joint angle variations; both of which persisted over time compared with control rats, suggestive of differences in the development and plasticity of locomotion over time and in the processing of somatosensory inputs (10) after SMR.

Children with CP exhibit reduced repertoires of movements and behavioral strategies that match an overall reduction in gait variation (24, 30). However, higher variation in cadence has been reported in children with CP (47), which leads invariably to delayed maturation of locomotion in older children with CP (8, 30). Interestingly, children with ASD also exhibit reduced postural stability and atypical gait, characterized by increased variations in stride length, posture and foot placement, reflecting impairments in the integration of somatosensory feedback (19, 41, 42, 60). In a recent model of encephalopathy of prematurity based on intrauterine hypoperfusion (14), prenatal ischemia led to increased gait variations over time, suggestive of adaptive strategy and/or a process of plasticity to increase the available repertoires of movements (17). Such a process is likely to delay gait maturation and/or to retain primitive reflexes and infantile gait features in children with CP and DCD (8, 30), and may reflect delays in the development of milestones and changes in muscle tone or spasticity (18, 24).

Musculoskeletal histopathology related to SMR

Postnatal movement restriction and enduring locomotion disorders significantly altered joint, bone and muscle structure. First, tibial length and bone density appeared reduced, and the knee joint cartilage showed moderate degenerative changes in adult SMR rats. Previously, we found greater articular damage and eburnations in the ankle than in the knee after SMR (15) that matched a persistent over-plantarflexion observed in all phases of stride. Comparable joint chondromalacia and muscle changes have been associated with gait abnormalities in patients with CP (32, 50). Joint abnormalities including chondromalacia in children with CP seem due to the imbalance in muscle forces across joints (38). Interestingly, SMR increased the weight load of the foot during weight support while footprint area was reduced, suggestive of unbalanced muscle forces.

Next, SMR induced marked reductions in the width, circumference, length and cross-sectional areas of the GS, suggestive of muscle atrophy. Comparable changes were observed in the rectus femoris and tibialis anterior muscles, indicating atrophy in several hind limb muscles after SMR. Rats undergoing similar SMR displayed smaller myofiber areas in the soleus plantarflexor muscle (34). Early hind limb unloading alters muscle phenotype toward a persistence of immature myofibers subtypes in the soleus muscle (43, 52). Taken together, these results demonstrate that early atypical motor experience degrades muscle structure and motor outputs, with enduring effects into adulthood.

Lastly, increased numbers of PAX7 immunopositive cells in SMR rats are indicative of increased regeneration or repair processes in the muscle (3, 17) and a response to the myofiber atrophy or constraint-induced injury (17). Hallmarks of fibrotic tissue after

muscle injury, including increased production of collagen type I and connective tissue growth factor (CTGF) were found after a similar SMR procedure (15). Although the GS tendon length was not altered by SMR, the muscle atrophy and shortened tibial bone correlated with the gait disturbances and corroborate the observations in children with spasticity (40, 62). We, thus, consider that the joint abnormalities were secondary changes related to an imbalance in muscle forces across the joints because of both atrophied myofibers in the various muscles acting on the knee and ankle (32, 38) and digitigrade locomotion after SMR. Such enduring musculoskeletal histopathology likely contributed to the emergence, persistence or aggravation of the gait and posture disorders in a self-perpetuating cycle.

SMR leads to muscle hyperreflexia

The presence of spasticity, hypertonicity, contractures or other-related clinical signs is usually caused by lesions of the CNS, such as spinal cord injury or stroke that disrupt information transmission to spinal motor networks in humans (18, 21, 22) or animal models (4, 5). Postnatal movement restriction induced increased stretch reflex and muscle hyperreflexia, indicative of spasticity and related muscle overactivity, even in the absence of brain damage. Thus, SMR induces hyperreflexia that appears related to enduring gait disorders, perturbations of the maturation of locomotion and various musculoskeletal pathologies, while the full range of passive motion of hind limb joints was preserved in SMR rats.

Abnormal proprioceptive feedback during limb disuse/immobilization after stroke leads to spasticity, contractures, hypertonicity, muscle atrophy and stiffness, various paresis and movement disturbances in humans (21, 22, 39). In the absence of brain damage, leg immobilization in adults leads to atrophy and reduced force development of the GS and clear signs of spasticity in the soleus (12, 13, 31). In the adult rat, 3 weeks of hind limb unloading increases the H-reflex gain (2). Recently, botulinum toxin-related abolishment of sensory feedback and motor commands leads to muscle atrophy and passive stiffness, maximal force reduction and increased stretch reflex in adult rats (45, 46). Taken together, these studies emphasize the deleterious impact of abnormal somatosensory feedback on the emergence of spasticity, muscle overactivities and related movement impairments.

Functional implications

Based on our results, we postulate that limited amounts quantity and abnormal patterns (quality) of movements during postnatal hind limb immobilization provide atypical sensorimotor experience that is likely at the origin of subsequent locomotor disorders, increased stretch reflex and musculoskeletal tissue degradation compared with controls (Figure 6). First, such an interplay between these features in relation to neural plasticity has been shown, although the degree and direction of causality is still in debate (8, 16, 18, 21, 22, 49). We can infer the existence of a self-perpetuating cycle, in which musculoskeletal pathologies may contribute to or exacerbate the degradation of locomotion and muscle overactivity. In turn, spasticity and related muscle disorders likely participate in musculoskeletal and locomotion disturbances (Figure 6). Second, we postulate that degraded movements because of impaired gait and spastic muscles provide atypical somatosensory

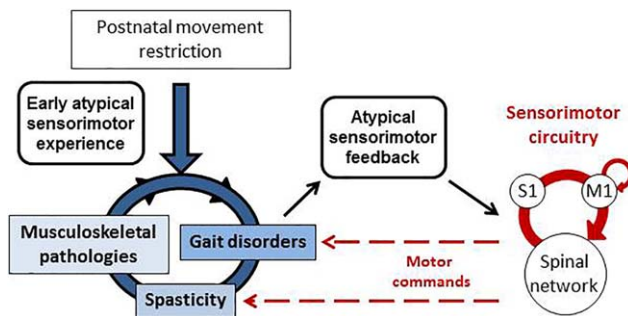


Figure 6. Schematic illustration of the deleterious impact of postnatal movement restriction on gait, musculoskeletal tissues and stretch reflex. Movement restriction during postnatal hind limb immobilization provides early atypical sensorimotor experience that leads to gait disorders, musculoskeletal pathologies and signs of spasticity. In turn, gait disorders and spastic muscles provides atypical sensorimotor feedback to the immature sensorimotor circuitry, mainly the spinal network and the primary somatosensory (S1) and motor (M1) cortices that intercommunicate. Such an atypical somatosensory feedback likely degrades the functional organization of S1 and M1 maps and of the spinal network, thus providing abnormal motor commands that finally aggravate gait disorders, spasticity and musculoskeletal abnormalities in a self-perpetuating cycle.

reafference to the immature sensorimotor circuitry, including primary somatosensory (S1) and motor (M1) cortices connected to other subcortical structures in the sensorimotor loop (55). We assume that this atypical somatosensory reafference degrades the functional organization of the S1 and M1 maps, as previously described (15, 54). Such atypical somatosensory reafference also effects the organization of the lumbar spinal cord circuitry, involved in both the motor command of automatic locomotion and the emergence of muscle overactivity and paresis (Figure 6) (8, 30). Indeed, the functional degradation of the sensorimotor circuitry may in turn produce altered motor commands, for example, abnormal muscle synergies observed in rats after hind limb unloading (6, 7) or in patients with CP (53). Further studies are needed to investigate the impact of early movement restriction or disuse on the functional reorganization in the sensorimotor cortex and lumbar spinal cord to gain new insights into the plastic processes underpinning the emergence of such disorders and pathologies.

The present study illustrates the crucial involvement of postnatal sensorimotor experience and somatosensory feedback in the development and persistence of abnormal movements in invalidating diseases with brain damage such as CP or without brain damage in the case of DCD or ASD. Our study emphasizes a likely self-perpetuating cycle, in which the lack of appropriate sensorimotor inputs during postnatal development exacerbates the initial deficit. We think these results have key implications for designing effective, positive and idiosyncratic interventions and physical activities, not only for promoting recovery from brain injury (21, 22, 36, 58), but also for preventing the secondary consequences of the sensorimotor circuitry disorganization, paresis and abnormal movement-related feedback that may result from atypical motor development either after brain damage in the case of CP, but also in ASD, DCD or other neurodevelopmental disorders without CNS injury.

ACKNOWLEDGMENTS

The authors are grateful to Prof J-M Graciès, L Bensoussan, V Triffreau and Drs M Kerzoncuf and F Boubred for helpful discussions and comments on the manuscript. The authors are thankful to Dr P. Marino (NSRepair, INT, Marseille) for his contribution to the Supporting Information Figure S1. The authors also wish to dedicate this work to Vicky Massicotte and Laurent Vinay, great neuroscientists recently deceased. This work was supported by the Centre National de la Recherche Scientifique (CNRS), the National Institute of Mental Health of the National Institutes of Health (Award Number P30 MH092177), Ministère de l'Enseignement Supérieur et de la Recherche, la Fondation Motrice, la Fondation NRJ-Institut de France, Région Provence-Alpes-Côte-d'Azur, the Cerebral Palsy Alliance, Temple University and Aix-Marseille Université. The authors have no conflicts of interest to declare.

REFERENCES

1. Akay T, Tourtellotte WG, Arber S, Jessell TM (2014) Degradation of mouse locomotor pattern in the absence of proprioceptive sensory feedback. *Proc Natl Acad Sci U S A* **111**:16877–16882.
2. Anderson J, Almeida-Silveira MI, Perot C (1999) Reflex and muscular adaptations in rat soleus muscle after hindlimb suspension. *J Exp Biol* **202**:2701–2707.
3. Bischoff R (1994) The satellite cell and muscle regeneration. In: *Myology*. AG Engel, C Franzini-Armstrong (eds), pp. 97–118. McGraw-Hill: New York.
4. Bos R, Sadlaoud K, Boulenguez P, Buttigieg D, Liabeuf S, Brocard C *et al* (2013) Activation of 5-HT_{2A} receptors upregulates the function of the neuronal K-Cl cotransporter KCC2. *Proc Natl Acad Sci U S A* **110**:348–353.
5. Boulenguez P, Liabeuf S, Bos R, Bras H, Jean-Xavier C, Brocard C *et al* (2010) Down-regulation of the potassium-chloride cotransporter KCC2 contributes to spasticity after spinal cord injury. *Nat Med* **16**:302–307.
6. Canu MH, Falempin M (1996) Effect of hindlimb unloading on locomotor strategy during treadmill locomotion in the rat. *Eur J Appl Physiol* **74**:297–304.
7. Canu M-H, Garnier C, Lepoutre F-X, Falempin M (2005) A 3D analysis of hindlimb motion during treadmill locomotion in rats after a 14-day episode of simulated microgravity. *Behav Brain Res* **157**:309–321.
8. Cappellini G, Ivanenko YP, Martino G, MacLellan MJ, Sacco A, Morelli D *et al* (2016) Immature spinal locomotor output in children with cerebral palsy. *Front Physiol* **7**:478.
9. Caron G, Marqueste T, Decherchi P (2016) Restoration of post-activation depression of the H-reflex by treadmill exercise in aged rats. *Neurobiol Aging* **42**:61–68.
10. Chau T, Young S, Redekop S (2005) Managing variability in the summary and comparison of gait data. *J NeuroEngineering Rehabil JNER* **2**:22–20.
11. Chinello A, Di Gangi V, Valenza E (2016) Persistent primary reflexes affect motor acts: potential implications for autism spectrum disorder. *Res Dev Disabil* **16**:30154–30158.
12. Clark BC, Fernhall B, Ploutz-Snyder LL (2006) Adaptations in human neuromuscular function following prolonged unweighting: I. Skeletal muscle contractile properties and applied ischemia efficacy. *J Appl Physiol* **101**:256–263.
13. Clark BC, Manini TM, Bolanowski SJ, Ploutz-Snyder LL (2006) Adaptations in human neuromuscular function following prolonged unweighting: II. Neurological properties and motor imagery efficacy. *J Appl Physiol* **101**:264–272.

14. Coq J-O, Delcour M, Massicotte VS, Baud O, Barbe MF (2016) Prenatal ischemia deteriorates white matter, brain organization, and function: implications for prematurity and cerebral palsy. *Dev Med Child Neurol* **58**:7–11.
15. Coq J-O, Strata F, Russier M, Safadi FF, Merzenich MM, Byl NN *et al* (2008) Impact of neonatal asphyxia and hind limb immobilization on musculoskeletal tissues and S1 map organization: implications for cerebral palsy. *Exp Neurol* **210**:95–108.
16. Damiano DL, Laws E, Carmines DV, Abel MF (2006) Relationship of spasticity to knee angular velocity and motion during gait in cerebral palsy. *Gait Posture* **23**:1–8.
17. Delcour M, Russier M, Xin DL, Massicotte VS, Barbe MF, Coq J-O (2011) Mild musculoskeletal and locomotor alterations in adult rats with white matter injury following prenatal ischemia. *Int J Dev Neurosci* **29**:593–607.
18. Dietz V, Sinkjaer T (2007) Spastic movement disorder: impaired reflex function and altered muscle mechanics. *Lancet Neurol* **6**:725–733.
19. Du W, Wilmut K, Barnett AL (2015) Level walking in adults with and without developmental coordination disorder: an analysis of movement variability. *Hum Mov Sci* **43**:9–14.
20. Einspieler C, Peharz R, Marschik PB (2016) Fidgety movements – tiny in appearance, but huge in impact. *J Pediatr (Rio J)* **92**:S64–S70.
21. Gracies J-M (2005) Pathophysiology of spastic paresis. I: paresis and soft tissue changes. *Muscle Nerve* **31**:535–551.
22. Gracies J-M (2005) Pathophysiology of spastic paresis. II: emergence of muscle overactivity. *Muscle Nerve* **31**:552–571.
23. Hadders-Algra M (2007) Putative neural substrate of normal and abnormal general movements. *Neurosci Biobehav Rev* **31**:1181–1190.
24. Hadders-Algra M (2010) Variation and variability: key words in human motor development. *Phys Ther* **90**:1823–1837.
25. Hadders-Algra M (2014) Early diagnosis and early intervention in cerebral palsy. *Front Neurol* **5**:185.
26. Hausdorff JM, Zemani L, Peng C-K, Goldberger AL (1999) Maturation of gait dynamics: stride-to-stride variability and its temporal organization in children. *J Appl Physiol* **86**:1040–1047.
27. Kerzencuf M, Bensoussan L, Delarque A, Durand J, Viton J-M, Rossi-Durand C (2015) Plastic changes in spinal synaptic transmission following botulinum toxin A in patients with post-stroke spasticity. *J Rehabil Med* **47**:910–916.
28. Khalki L, Ba M'hamed S, Sokar Z, Bennis M, Vinay L, Bras H *et al* (2013) Prenatal exposure to fenugreek impairs sensorimotor development and the operation of spinal cord networks in mice. *PLoS One* **8**:e80013.
29. Lee S, Toda T, Kiyama H, Yamashita T (2014) Weakened rate-dependent depression of Hoffmann's reflex and increased motoneuron hyperactivity after motor cortical infarction in mice. *Cell Death Dis* **5**:e1007.
30. Leonard C, Hirschfeld H, Forssberg H (1988) Gait acquisition and reflex abnormalities in normal children and children with cerebral palsy. In: *Posture Gait Dev. Adapt. Modul. Proc. 9th Int. Symp. Postural Gait Res. Marseille Fr.* B Amblard, A Berthoz, F Clarac (eds), pp. 33–45. Excerpta Medica: Amsterdam.
31. Lundbye-Jensen J, Nielsen JB (2008) Immobilization induces changes in presynaptic control of group Ia afferents in healthy humans. *J Physiol* **586**:4121–4135.
32. Marbini A, Ferrari A, Cioni G, Bellanova MF, Fusco C, Gemignani F (2002) Immunohistochemical study of muscle biopsy in children with cerebral palsy. *Brain Dev* **24**:63–66.
33. Marcroft C, Khan A, Embleton ND, Trenell M, Plötz T (2015) Movement recognition technology as a method of assessing spontaneous general movements in high risk infants. *Neuropediatrics* **5**:284.
34. Marcuzzo S, Ferreira Dutra M, Stigger F, Severo do Nascimento P, Ilha J, Kalil-Gaspar PI *et al* (2008) Beneficial effects of treadmill training in a cerebral palsy-like rodent model: walking pattern and soleus quantitative histology. *Brain Res* **1222**:129–140.
35. Marcuzzo S, Dutra MF, Stigger F, do Nascimento PS, Ilha J, Kalil-Gaspar PI *et al* (2010) Different effects of anoxia and hind-limb immobilization on sensorimotor development and cell numbers in the somatosensory cortex in rats. *Brain Dev* **32**:323–331.
36. Merzenich MM, Van Vleet TM, Nahum M (2014) Brain plasticity-based therapeutics. *Front Hum Neurosci* **8**:385.
37. Moreau NG, Simpson KN, Teeffey SA, Damiano DL (2010) Muscle architecture predicts maximum strength and is related to activity levels in cerebral palsy. *Phys Ther* **90**:1619–1630.
38. Morrell DS, Pearson JM, Sauter DD (2002) Progressive bone and joint abnormalities of the spine and lower extremities in cerebral palsy. *Radiogr Rev Publ Radiol Soc N Am Inc* **22**:257–268.
39. Narici MV, de Boer MD (2011) Disuse of the musculo-skeletal system in space and on earth. *Eur J Appl Physiol* **111**:403–420.
40. Oeffinger D, Conaway M, Stevenson R, Hall J, Shapiro R, Tytkowski C (2010) Tibial length growth curves for ambulatory children and adolescents with cerebral palsy. *Dev Med Child Neurol* **52**:e195–e201.
41. Parma V, de Marchena AB (2016) Motor signatures in autism spectrum disorder: the importance of variability. *J Neurophysiol* **115**:1081–1084.
42. Phagava H, Muratori F, Einspieler C *et al* (2008) General movements in infants with autism spectrum disorders. *Georgian Med News* **100**–105.
43. Picquet F, Stevens L, Butler-Browne GS, Mounier Y (1998) Differential effects of a six-day immobilization on newborn rat soleus muscles at two developmental stages. *J Muscle Res Cell Motil* **19**:743–755.
44. Pieters S, De Block K, Scheiris J, Eyssens M, Desoete A, Deboutte D *et al* (2012) How common are motor problems in children with a developmental disorder: rule or exception?. *Child Care Health Dev* **38**:139–145.
45. Pingel J, Hultborn H, Näslund-Koch L, Jensen DB, Wienecke J, Nielsen JB (2017) Muscle disuse caused by botulinum toxin injection leads to increased central gain of the stretch reflex in the rat. *J Neurophysiol* **118**:1962–1969.
46. Pingel J, Wienecke J, Lorentzen J, Nielsen JB (2016) Botulinum toxin injection causes hyper-reflexia and increased muscle stiffness of the triceps surae muscle in the rat. *J Neurophysiol* **116**:2615–2623.
47. Prosser LA, Lauer RT, VanSant AF, Barbe MF, Lee SCK (2010) Variability and symmetry of gait in early walkers with and without bilateral cerebral palsy. *Gait Posture* **31**:522–526.
48. Riesenfeld A (1972) Metatarsal robusticity in bipedal rats. *Am J Phys Anthropol* **36**:229–233.
49. Rodda JM, Graham HK, Carson L, Galea MP, Wolfe R (2004) Sagittal gait patterns in spastic diplegia. *J Bone Joint Surg Br* **86**:251–258.
50. Rose J, Haskell WL, Gamble JG, Hamilton RL, Brown DA, Rinsky L (1994) Muscle pathology and clinical measures of disability in children with cerebral palsy. *J Orthop Res off Publ Orthop Res Soc* **12**:758–768.
51. Rosenbaum P, Paneth N, Leviton A, Goldstein M, Bax M, Damiano D *et al* (2007) A report: the definition and classification of cerebral palsy April 2006. *Dev Med Child Neurol Suppl* **109**:8–14.
52. Serradj N, Picquet F, Jamon M (2013) Early postnatal motor experience shapes the motor properties of C57BL/6J adult mice. *Eur J Neurosci* **38**:3281–3291.
53. Steele KM, Rozumalski A, Schwartz MH (2015) Muscle synergies and complexity of neuromuscular control during gait in cerebral palsy. *Dev Med Child Neurol* **57**:1176–1182.
54. Strata F, Coq JO, Byl N, Merzenich MM (2004) Effects of sensorimotor restriction and anoxia on gait and motor cortex organization: implications for a rodent model of cerebral palsy. *Neuroscience* **129**:141–156.

55. Tiriác A, Blumberg MS (2016) Gating of reafference in the external cuneate nucleus during self-generated movements in wake but not sleep. *Elife* **5**:e18749.
56. Tiriác A, Sokoloff G, Blumberg MS (2015) Myoclonic twitching and sleep-dependent plasticity in the developing sensorimotor system. *Curr Sleep Med Rep* **1**:74–79.
57. Vaivre-Douret L, Lalanne C, Golse B (2016) Developmental coordination disorder, an umbrella term for motor impairments in children: nature and co-morbid disorders. *Front Psychol* **7**:e502.
58. Verschuren O, Peterson MD, Balemans ACJ, Hurvitz EA (2016) Exercise and physical activity recommendations for people with cerebral palsy. *Dev Med Child Neurol* **58**:798–808.
59. Walton KD, Lieberman D, Llinás A, Begin M, Llinás RR (1992) Identification of a critical period for motor development in neonatal rats. *Neuroscience* **51**:763–767.
60. Wang Z, Magnon GC, White SP, Greene RK, Vaillancourt DE, Mosconi MW (2015) Individuals with autism spectrum disorder show abnormalities during initial and subsequent phases of precision gripping. *J Neurophysiol* **113**:1989–2001.
61. Westerga J, Gramsbergen A (1993) The effect of early movement restriction: an EMG study in the rat. *Behav Brain Res* **59**:205–209.
62. Wren TAL, Cheatwood AP, Rethlefsen SA, Hara R, Perez FJ, Kay RM (2010) Achilles tendon length and medial gastrocnemius architecture in children with cerebral palsy and equinus gait. *J Pediatr Orthop* **30**:479–484.

SUPPORTING INFORMATION

Additional Supporting Information may be found in the online version of this article at the publisher's web-site:

Table S1. Averaged kinematic parameters in controls and rats that underwent postnatal SMR at different ages (P30 and P65) for a treadmill speed of 0.23 m/s. The footprint surface area and weight load during the stance was also measured at P30. To ease clarity, bold numbers point out differences between SMR and control rats at the same age.

Figure S1. Illustration of the electrophysiological techniques used to measure the H-reflex in the flexor digitorum of adult rats. **A.** Schematic description of the reflex loop and the elicitation of the M wave and H-reflex by the electric stimulation of

the sensorimotor nerve. Adapted from Lee *et al.*, 2014. **B.** Illustration of the set up that includes stimulating electrodes inserted in the tibial nerve about 1 cm above the ankle, recording electrodes implanted subcutaneously in the flexor digitorum brevis (FDB) and a reference electrode inserted in the skin of the tail. The black thermal pad to maintain rat's temperature around 37°C is also shown, but not the rectal probe that control the thermal pad. The distance between the pairs of recording and stimulating electrodes has been optimized to well differentiate the M wave from the H signal, as shown in **A.**

Figure S2. Morphological assessment of the femoral and knee joints in controls and rats exposed to postnatal sensorimotor restriction (SMR). Numbers in panels **A** and **B** represent the scoring zones used for the Mankin evaluation (see text and Figure 3D,E). **A.** Control knee at low power showing normal staining of articular cartilages and well defined basophilic tidemarks. **B.** A SMR knee, which even at low power, displays a general loss of the cartilage tidemark, a basophilic line marking the boundary between calcified matrix and uncalcified cartilage. **C.** Control tibial cartilage showing normal organization of chondrocytes into isogenous groups and normal size lacuna. All but one of the blood vessels (indicated by an arrow) are located away from the edge of the soft cartilage (indicated by a clear tidemark region separating the lightly stained cartilage matrix from the dark pink stained calcified matrix). **D.** SMR tibial cartilage showing chondrocytes which displayed hypercellularity and clustering, as depicted by arrows. **E.** High power magnification of a femur in a restrained rat showing a loss of articular cartilage. **F.** High power magnification of tibial bone in a SMR rat showing the abnormal epiphyseal growth plate. **G.** Total Mankin score of both structural and cellular changes are shown for zones 1–3. Mean \pm SEM. * $P < 0.05$, compared with controls; ** $P < 0.01$, compared with controls. Cont = Controls; F = Femur; M = Meniscus; T = Tibia. Scale bars are indicated.

Video Clip S1. Gait and posture in an illustrative control rat at P25.

Video Clip S2. Example of movement and posture impairments related to knee and ankle hyperextension in a representative SMR rat at P25.